J Fluoresc (2015) 25:1417–1429
DOI 10.1007/s10895-015-1632-z

ORIGINAL ARTICLE

Fluorescence Behaviour and Singlet Oxygen Production of Aluminium Phthalocyanine in the Presence of Upconversion Nanoparticles

Zane Watkins[1] · Jessica Taylor[1] · Sarah D'Souza[1] · Jonathan Britton[1] · Tebello Nyokong[1]

Received: 23 May 2015 / Accepted: 26 July 2015 / Published online: 13 August 2015

Abstract $NaYF_4$:Yb/Er/Gd upconversion nanoparticles (UCNP) were synthesised and the photoemission stabilised by embedding them in electrospun fibers. The photophysical behaviour of chloro aluminium tetrasulfo phthalocyanine (ClAlTSPc) was studied in the presence of UCNPs when the two are mixed in solution. The fluorescence quantum yield value of ClAlTSPc decreased in the presence of UCNPs due to the heavy atom effect of UCNPs. This effect also resulted in increase in triplet quantum yields for ClAlTSPc in the presence of UCNPs. The fluorescence lifetimes for UCNPs were shortened at 658 nm in the presence of ClAlTSPc when the former was embedded in fiber and suspended in a dimethyl sulfoxide solution of the latter. A clear singlet oxygen generation by ClAlTSPc though Förster resonance energy transfer was demonstrated using a singlet oxygen quencher, 1,3-diphenylisobenzofuran.

Keywords Upconversion nanoparticles · Aluminium tetrasulfo phthalocyanine · Fluorescence quantum yields · Triplet quantum yields · Electrospun fibers

Introduction

Phthalocyanines (Pcs) have been extensively studied due to their vast range of applications. These include as dyes, colorants, non-linear optical materials, photoconductors, solar energy conversion platforms and active centres for sensing applications [1–5]. What makes them so attractive is their high chemical and photo stability as well as the ease of alteration of their central metals and peripheral substituents, making them incredibly diverse [6, 7]. Pcs also have very promising uses in the medical fields such as in photodynamic therapy (PDT) [8–10]. Pcs are useful as PDT photosensitising agents because they have the ability to accumulate in tumors and produce singlet oxygen once excited by light [6, 11–13]. There are however challenges facing Pcs as photosensitizers, such as limited cell penetration depth [6] and low solubility. These shortcomings may be overcome by creation of multifunctional nano systems which makes use of a variety of properties from different materials [14].

Upconversion nanoparticles (UCNP) convert low energy into higher energy. UCNPs usually come in the form of lanthanide doped nanomaterials. These particles exhibit unique photochemical properties such as high resistance to photobleaching and photodegredation, non-blinking, high chemical stability, sharp emission bands, near infrared (NIR) excitation, large anti stokes emissions, no auto fluorescence from biological samples, large penetration depth and an easy separation of emission peaks [15–18].

The most prevalent form of upconversion nanoparticles (UCNPs) are the rare-earth fluoride nanocrystals, these typically appear as the $NaYF_4$ host lattices, co-doped with the trivalent lanthanides Er^{3+} and Yb^{3+} [14, 15]. UCNPs fluoresce in the visible region of the electromagnetic spectrum typically at the blue, green and red. These emissions can also be tuned selectively depending on the dopant lanthanides [15, 19].

The NIR absorption (at~980 nm) of the UCNPs falls within the biological window of light penetration, meaning that they can absorb light in deeper regions of the body, limiting damage to tissues and extending the range of cancer treatment [14, 19].

✉ Tebello Nyokong
t.nyokong@ru.ac.za

[1] Department of Chemistry, Rhodes University, P.O. Box 94, Grahamstown, South Africa

The UCNPs employed in this work are $NaYF_4$:Yb/Er/Gd nanoparticles. To improve solubility and for future linking of the UCNPs to the phthalocyanines, $NaYF_4$:Yb/Er/Gd UCNPs were functionalized with a silica shell using tetraethyl orthosilicate (TEOS) to give $NaYF_4$:Yb/Er/Gd@Si, Scheme 1. This was followed by the addition of 3-aminopropyl triethoxy silane (APTES) to give amino containing UCNPs represented as $NaYF_4$:Yb/Er/Gd@Si@NH_2, Scheme 1.

For practical applications, UCNPs with high upconversion efficiency, bright luminescence, and good colloidal stability are desirable. This has been achieved by incorporating UCNPs into crystals [20]. Encapsulation of the UCNPs with polyethylene glycol (PEG)-phospholipid was found to be effective in retaining both upconversion luminescence intensity and dispersibility in aqueous environment [21]. $NaYF_4$:Yb/Er nanocrystals have been electrospun in SiO_2 composite fibres, poly(methyl methacrylate) (PMMA) and PCL-gelatin composite fibres for an array of applications, displaying characteristics such as emission enhancement and improved drug delivery [22–24], hence electrospun fibers are employed in this work in order to achieve stable fluorescence and improved upconversion efficiency. The UCNPs at different capping stages are mixed with a polystyrene polymer solution and spun into nanofibers. For studies on the effects of chloro aluminium tetraphthalocyanine (ClAlTSPc, Fig. 1) on the fluorescence behaviour of UCNPs, the electrospun fibers containing UCNPs were suspended in a solution of ClAlTSPc in dimethyl sulfoxide (DMSO). The UCNPs were best studied when embedded in fibers (not in solution) in order to obtain a stable UCNPs fluorescence signal. Figure 1 shows a photo of a UV–vis cell

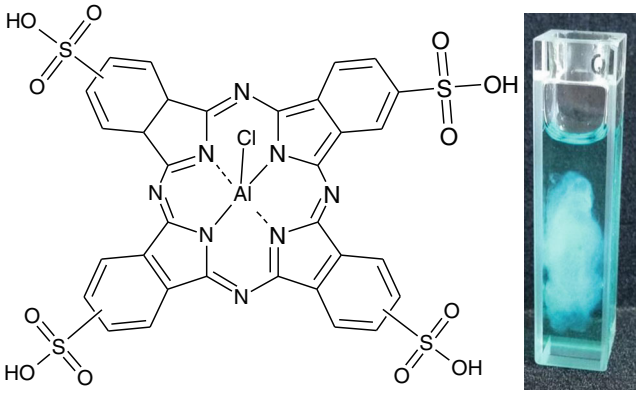

Fig. 1 Structure of ClAl tetra sulfophthalocyanine and a photo of electrospun fiber embedded in ClAlTSPc solution (in DMSO)

containing electrospun fiber containing UCNPs embedded in ClAlTSPc solution. The photophysical properties of ClAlTSPc in the presence of UCNPs were evaluated when both are in DMSO solution (ie UCNPs not embedded in electrospun fibers). For the study of singlet oxygen generating abilities of ClAlTSPc in the presence of UCNPs, the latter were embedded in fiber in order to stabilise the UCNPs luminescence. UCNPs act as nanotransducers, absorbing NIR light and transferring the energy to ClAlTSPc [25] through Förster resonance energy transfer (FRET).

There have been some studies on the nanocomposites of phthalocyanines with UCNPs, but concentrating on the singlet oxygen generation by the Pcs upon excitation of UCNPs [26, 27]. Silicon phthalocyanine dihydroxide ((OH) $_2$SiPc) has been covalently linked to UCNPs [26]. Excitation where UCNPs absorb (980 nm) resulted in energy transfer to ((OH) $_2$SiPc) and the generation of singlet

Scheme 1 Schematic of UCNP capping and functionalisation

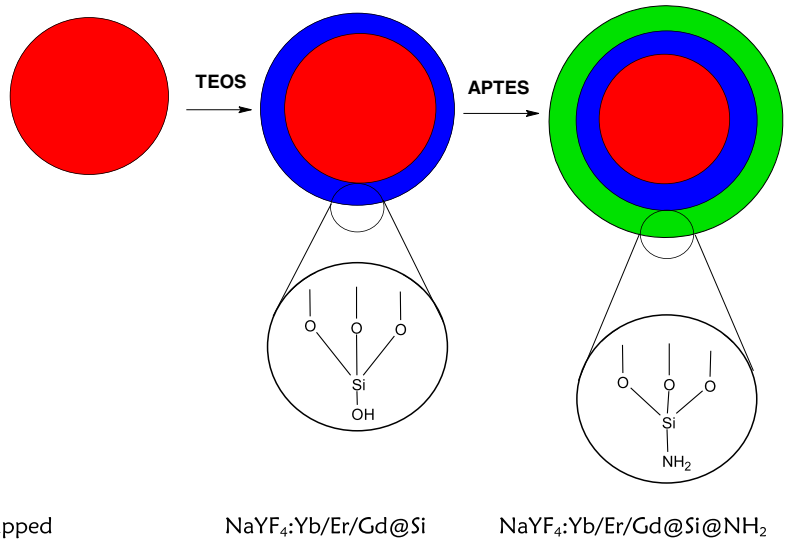

oxygen [26]. Tetrasubstituted carboxy aluminum phthalocyanine has been covalently linked to silica-coated $NaGdF_4$:Yb,Er/$NaGdF_4$ nanoparticles and applied in photodynamic therapy (PDT) and magnetic resonance imaging (MRI) of cancer cells. The conjugate was found to be efficient in generating cytotoxic singlet oxygen under near-infrared (NIR) light irradiation [27]. This is the first time that the effects of UCNPs on the fluorescence and triplet state behaviour of ClAlTSPc are studied. In addition to the effects of the ClAlTSPc on the fluorescence behaviour of UCNPs are presented.

Experimental

Materials

The lanthanide salts and various other salts used were provided by Sigma Aldrich and they include: $Y(NO_2)_3.(H_2O)_6$, $ErCl_3.(H_2O)_6$, $YbCl_3.(H_2O)_6$, $GdCl_3.(H_2O)_6$, NH_4F and NaOH pellets. Sigma Aldrich also provided tetraethylorthosilicate (TEOS), Igepal CO-520, 1-octadecene, oleic acid, 3-aminopropyltriethoxysilane (APTES), polystyrene (PS, Mw=192,000 g/mol) and 1, 3-diphenylisobenzofuran (DPBF). Solvents such as ethanol (EtOH), methanol (MeOH), toluene, thionyl chloride, dimethylformamide (DMF), tetrahydrofuran (THF), dimethyl sulfoxide (DMSO) and cyclohexane were from SAARCHEM. Aluminium tetrasulfophthalocyanine (Fig. 1) was synthesized in accordance with literature [28].

Equipment

The thermal decomposition reactions were undertaken in a rotary regavolt temperature controlled Gallenkamp porcelain heating oven. UCNPs were washed and collected with a Merk chemicals Eppendorf Centrifuge 5810. Ground-state electronic absorption spectra were recorded on a Shimadzu, UV–vis 2550 spectrometer. Excitation and emission spectra were recorded using a Varian Eclipse fluorescence spectrofluorimeter. Transmission electron microscopy (TEM) images were obtained using a JEOL JEM 1210 transmission electron microscope using 90 KW acceleration voltage. Scanning electron microscope (SEM) images of the fibre alone or modified with UCNPs were obtained using a JOEL JSM 840 scanning electron microscope.

Powder X-ray diffraction (XRD) spectra were performed on a Bruker D8 Discover diffractometer, equipped with a Lynx Eye detector, under Cu-Kα radiation (λ=1.5405 Å). Data were collected in the range from 2θ=10° to 100°, scanning at 0.010° min^{-1} and 192 s per step. The samples were placed on a zero background silicon wafer slide.

For time correlated single photon counting (TCSPC) studies, the UCNPs were excited at 975 nm with a diode laser (LDH-D-C-980, burst mode, 40 MHz repetition rate, PicoQuant GmbH). The detector employed was a Peltier cooled Photomultiplier (PMA-C 192-M, PicoQuant GmbH) for both fluorescence spectra and lifetime studies. For excitation of the ClAlTSPc, the excitation source was a diode laser (LDH-P-670 driven by PDL 800-B, 670 nm, 20 MHz repetition rate, 44 ps pulse width, Picoquant GmbH). NIR spectrum of UCNPs was recorded on a Varian 500 UV–Vis/NIR spectrophotometer.

A laser flash photolysis system was used for the determination of triplet decay kinetics. The excitation pulses were produced by a tuneable laser system consisting of Nd:YAG laser (355 nm, 135 mJ/4–6 ns), pumping an optical parametric oscillator (OPO, 30 mJ/ 3–5 ns) with a wavelength range from 420 to 2300 nm (NT-342B, Ekspla). Triplet lifetimes were determined by the exponential fitting of the kinetic curves using the Origin 8 Professional software. The absorbance used for triplet state studies was kept at 1.5 and the solutions were degassed by bubbling argon for 30 min prior to measurements.

Synthesis of Upconversion Nanoparticles

Uncapped $NaYF_4$:Yb/Er/Gd

The UCNPs were synthesised as reported in literature [29] with slight modification as follows: the lanthanide salts consisting of $ErCl_3.(H_2O)_6$ (0.0061 g, 0.016 mmol), $YbCl_3.(H_2O)_6$ (0.0558 g, 0.144 mmol), $GdCl_3.(H_2O)_6$ (0.0441 g, 0.1186 mmol) and $Y(NO_2)_3.(H_2O)_6$, (0.1992 g and 0.595 mmol) were dispersed in 4 ml methanol and added to a mixture of oleic acid (6 ml) and 1-octadecene (4 ml) in a 100 ml round bottomed flask. The mixture was heated to 160 °C while stirring for 30 min. The solution was let to cool down to room temperature. NH_4F (0.1185 g, 2.2 mmol] and NaOH (0.08 g, 2 mmol) were added to 10 ml of methanol and sonicated until fully dispersed. This mixture was then added to the solution above and stirred at room temperature for 30 min. A 70 °C heating step took place for 30 min, to remove excess solvent, and then the mixture was cooled to room temperature. The solution was then heated to 300 °C for 90 min in a GallenKamp porcelain heating oven, with the temperature being monitored with an external thermocouple. The solution was flushed with argon for 30 min, before the heating began. After 90 min heating, the solution was cooled to room temperature and then washed with ethanol. The precipitate was collected by centrifuge for 20 min at 3000 rpm and then dried at 70 °C for 24 h. The resulting nanoparticles are termed uncapped $NaYF_4$:Yb/Er/Gd UCNPs.

Silica Capped $NaYF_4$:Yb/Er/Gd@Si

The uncapped $NaYF_4$:Yb/Er/Gd UCNPs (70 mg) prepared above, were dispersed in of cyclohexane (60 ml) in a round bottomed flask. Igepal CO-520 (1 ml), which acts as a surfactant for the facilitation of the silicon oxide layer, was added. After 5 min, a second portion of Igepal CO-520 (4 ml) and 0.92 ml of 30 % ammonia were added to facilitate the capping of the nanoparticles with a siliconoxide layer. The solution was sonicated until a transparent emulsion was obtained. TEOS (400 μl) was added dropwise and then the reaction mixture was left to stir for 4 days. The silica capped nanoparticles were then precipitated out with methanol, and then washed using a 1:1 EtOH and H_2O mixture. The nanoparticles were collected by centrifugation for 20 min at 3000 rpm and left to dry. The resulting nanoparticles are represented as $NaYF_4$:Yb/Er/Gd@Si UCNPs, Scheme 1. The $NaYF_4$:Yb/Er/Gd@Si UCNPs were washed with anhydrous ethanol followed by toluene.

Amino Capped $NaYF_4$:Yb/Er/Gd@Si@NH_2

The cleaned $NaYF_4$:Yb/Er/Gd@Si UCNPs (10 mg) were added to DMF (12 ml) and toluene (8 ml) in a 100 ml round bottomed flask and stirred for 10 min. APTES (1000 μl) was subsequently added drop-wise. The mixture was stirred for 24 h at room temperature under argon atmosphere. The particles were washed with toluene, methanol and then collected by centrifuge. The resulting nanoparticles are represented as $NaYF_4$:Yb/Er/Gd@Si@NH_2 UCNPs, Scheme 1.

Electrospinning

UCNPs (uncapped $NaYF_4$:Yb/Er/Gd, $NaYF_4$:Yb/Er/Gd@Si or $NaYF_4$:Yb/Er/Gd@Si@NH_2) (0.0013 g) were added to polystyrene (PS, 2.5 g) in a solvent mixture of DMF (8 ml) and THF (2 ml). The resulting solution was then stirred for 24 h at ambient temperature. After 24 h of stirring, the solution was deposited in a syringe. The height from the tip of the needle to the collector plate was set at 11 cm with the flow rate set up at 0.03 ml/h. The voltage between the collector plate and the needle tip was set to 15 kV. The set up was left running until a uniform looking electrospun fiber matt had formed. The UCNPs in the fibre are represented with PS (for polystyrene at the end). The UCNPs containing fibres are designated as uncapped $NaYF_4$:Yb/Er/Gd/PS, $NaYF_4$:Yb/Er/Gd@Si/PS and $NaYF_4$:Yb/Er/Gd@Si@NH_2/PS.

Forster Resonance Energy Transfer (FRET) Efficiency

FRET efficiencies (*Eff*) may be quantified from the fluorescence quantum yields or lifetimes of the donor in the absence ($\Phi_{F(UCNP)}$ or $\tau_{F(UCNP)}$) and the presence ($\Phi^{mixed}_{F(UCNP)}$ or $\tau^{mixed}_{F(UCNP)}$) of the acceptor, respectively using Eqs. 1 and 2 [30, 31].

$$Eff = 1 - \frac{\Phi^{linked}_{F(QD)}}{\Phi_{F(QD)}} \quad (1)$$

$$Eff = 1 - \frac{\tau^{mixed}_{F(QD)}}{\tau_{F(QD)}} \quad (2)$$

Equation 2 was employed in this work since fluorescence quantum yields could not be determined due to lack of standards.

Results and Discussion

Characterisation of UCNPs

Transmission Electron Microscopy Analysis

The uncapped $NaYF_4$:Yb/Er/Gd nanoparticles shown in Fig. 2a are roughly 40 nm in size, monodispersed and have a uniform hexagonal disc shape. The $NaYF_4$:Yb/Er/Gd@Si particles in Fig. 2b are clearly coated in a silica shell and exhibit monodisparity. The same cannot be said for the $NaYF_4$:Yb/Er/Gd@Si@NH_2, Fig. 2c which show aggregation. Figure 2d shows the TEM image of NaY_4:Yb/Er/Gd@Si@NH_2 following mixing with ClAlTSPc, showing less aggregation compared to NaY_4:Yb/Er/Gd@Si@NH_2 alone. The sizes for NaY_4:Yb/Er/Gd@Si@NH_2 and NaY_4:Yb/Er/Gd@Si were not too different from uncapped NaY_4:Yb/Er/Gd.

XRD Analysis

The XRD spectra, Fig. 3a, confirms that the particle size for uncapped $NaYF_4$:Yb/Er/Gd UCNP is roughly 40 nm, using the Debye Scherrer Eq. (3) [32],

$$d = \frac{k\lambda}{\beta\cos\theta} \quad (3)$$

where λ is the wavelength of the X-ray source (1.5405 Å), k is an empirical constant with a value of 0.9, β is the full width at half maximum of the diffraction peak, and θ is the angular position. The UCNP size of 40 nm confirms our findings obtained using TEM. The numbers above each peak are assigned to the crystal phase of the particles, which in this case is hexagonal. For $NaYF_4$:Yb/Er/Gd@Si (Fig. 3b) and $NaYF_4$:Yb/Er/Gd@Si@NH_2 (Fig. 3c), there is a large broad peak at the 2θ=20° which corresponds to the non-crystalline silica shell on the UCNP surface. Again the XRD spectra combined with TEM analysis further confirm that the silica

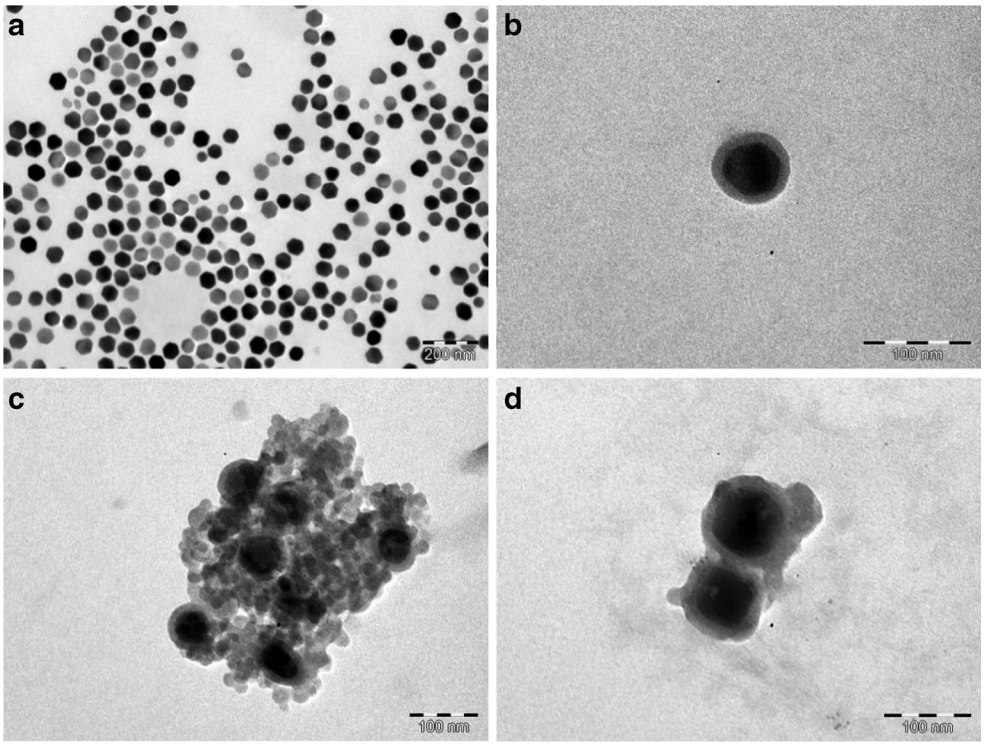

Fig. 2 TEM images of uncapped $NaYF_4$:Yb/Er/Gd UCNPs (**a**), $NaYF_4$:Yb/Er/Gd@Si UCNPs (**b**), $NaYF_4$:Yb/Er/Gd@Si@NH_2 (**c**) and $NaYF_4$:Yb/Er/Gd@Si@NH_2 mixed with ClAlTSPc (**d**)

or amino cappings had no effect on the crystal structure of the $NaYF_4$:Yb/Er/Gd hexagonal UCNP. No significant size difference was obtained between the different types of UCNPs using XRD.

Absorbance

Figure 4 (insert) shows the NIR absorbance for a typical $NaYF_4$:Yb/Er/Gd UCNP, which is within the biological window and not near where ClAlTSPc absorbs as will be discussed below. The UCNPs spectrum is in solution not in electrospun fiber, but gives an idea of the peak positions.

Spectral and Photophysical Behaviour of ClAlTSPc Alone or in the Presence of UCNPs: Excitation Where ClAlTSPc Absorbs

The studies in this section were done using a mixture of UCNPs (not embedded in fiber) and AlTSPc in solution, in order the check the effect of UCNPs on the spectral and photophysical behaviour of ClAlTSPc as explained in the introduction. For these studies it was not important to stabilize UCNPs in fiber (as will be done below) since it is the changes in the properties of ClAlTSPc (not UCNPs) being evaluated.

Absorbance and Fluorescence Spectra

Figure 4 shows that there was no change in the ClAlTSPc spectrum on addition of UCNPs. No change is expected since the latter absorbs at ~980 nm, and hence do not absorb where the Pc absorbs.

The absorption spectral maxima are the same as the excitation spectral maxima for ClAlTSPc alone and in the presence of UCNPs, Fig. 5. The emission spectra are mirror images of the excitation and absorption spectra.

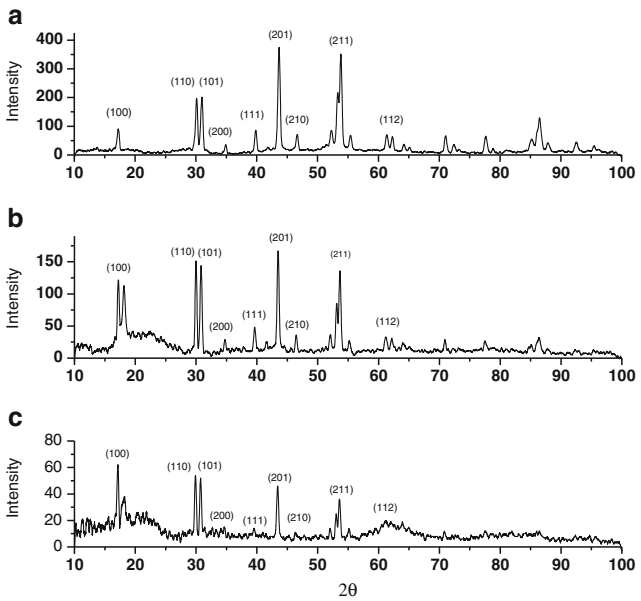

Fig. 3 XRD spectra for uncapped $NaYF_4$:Yb/Er/Gd (**a**) and $NaYF_4$:Yb/Er/Gd@Si (**b**) $NaYF_4$:Yb/Er/Gd@Si@NH_2 (**c**) UCNPs

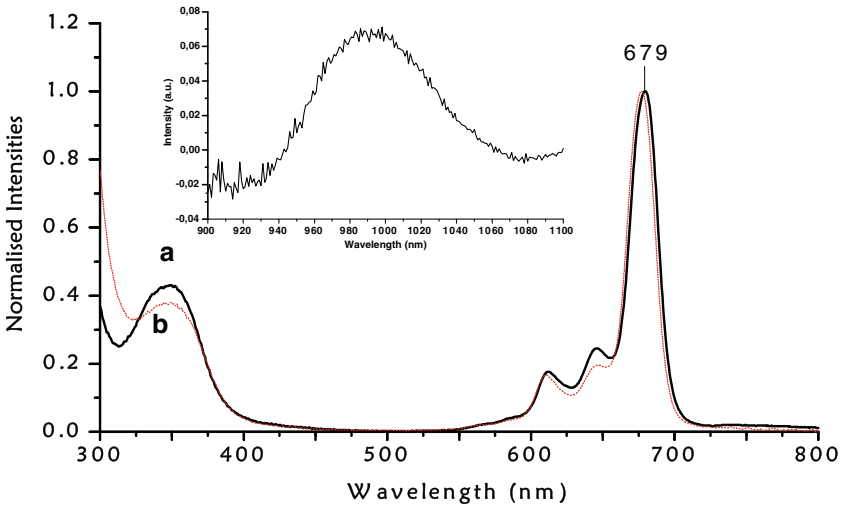

Fig. 4 UV–vis Absorption spectra of ClAlTSPc alone (7.3×10^{-6} M) (**a**) and in the presence of $NaYF_4$:Yb/Er/Gd@Si@NH_2 (**b**). Insert=NIR absorbance spectra for uncapped $NaYF_4$:Yb/Er/Gd UCNPs

Fluorescence Quantum Yields and Lifetimes

Fluorescence quantum yield of ClAlTSPc was determined in DMSO using Eq. 4 [33]:

$$\Phi_F = \Phi_{F(Std)} \frac{F.A_{Std}.n^2}{F_{Std}.A.n^2_{Std}} \quad (4)$$

where Φ_F is the quantum yield of the sample and $\Phi_{F(Std)}$ that of the standard ZnPc, $\Phi_{F(Std)}$ = 0.20 in DMSO [34], F and F_{std} represent the area under the fluorescence emission curve for the sample and standard, respectively; A and A_{std} refer to the absorbance of the sample and standard, respectively and n and n_{Std} are the refractive indices of the sample and standard solutions, respectively. The samples and the standard were both excited at the same relevant wavelength in each case. Excitation was where UCNPs do not absorb and Pcs do.

In Table 1, the Φ_F value of ClAlTSPc in the presence of UCNPs decreases due to the heavy atom effect of the latter, which encourages intersystem crossing to the triplet state rather than fluorescence. Figure 6 shows the TCSPC traces of ClAlTSPc in the absence and presence of $NaYF_4$:Yb/Er/Gd@Si@NH_2. Fluorescence lifetimes are longer for ClAlTSPc in the presence of UCNPs and could be due to the protection of the former by the latter from the environment.

Triplet State Behaviour

The triplet decay curves for ClAlTSPc alone and in the presence of UCNPs are shown in Fig. 7. The data was fitted to a monoexponential decay for ClAlTSPc alone or in the presence of UCNPs. Triplet quantum yields of the ClAlTSPc alone or in the presence of UCNPs were determined by the comparative method, using Eq. 5.

$$\Phi_T = \Phi_T^{Std} \frac{\Delta A_T \varepsilon_T^{Std}}{\Delta A_T^{Std} \varepsilon_T} \quad (5)$$

where ΔA_T and ΔA_T^{Std} are the changes in the triplet state absorption of the MPc derivative and the standard (ZnPc), respectively. Φ_T^{Std} is the triplet state quantum yield for the standard (Φ_T^{Std} = 0.65 for ZnPc in DMSO [35]). ε_T and ε_T^{Std} are the triplet state extinction coefficients for the MPc derivatives and the standard, respectively.

The triplet quantum yield for ClAlTSPc alone was taken from literature [36]. Higher triplet quantum yields are expected (and observed) for ClAlTSPc in the presence of UCNPs as a result of heavy atoms associated with UCNPs which encourages intersystem crossing to the triplet state, Table 1. The triplet lifetimes for ClAlTSPc became longer in the presence of UCNPs, Table 1. Lengthening of triplet lifetimes of Pcs in the presence of nanoparticles (such as quantum dots) has been observed before [37] and was attributed to the protection of the Pc by the nanoparticles. This could also be the reason for the lengthening of triplet lifetimes of ClAlTSPc in the presence of UCNPcs.

Photophysical Behaviour of UCNPs Alone or in the Presence of ClAlTSPc: Excitation Where UCNPs Absorb (at 975 nm)

Fluorescence of UCNPs Alone in Solution (not in Fiber)

These studies were done in ethanol and DMSO, except for uncapped UCNPs alone which were not soluble in ethanol. Fluorescence analysis of the hexagonal discs produced typical emission peaks associated with UCNPs, Fig. 8. The fluorescence exhibited by the UCNPs following excitation at 975 nm, is characteristic, with peaks in the red (~658 nm) and green (~540 nm) area of the electromagnetic spectrum indicating steady upconversion properties. In solution (both

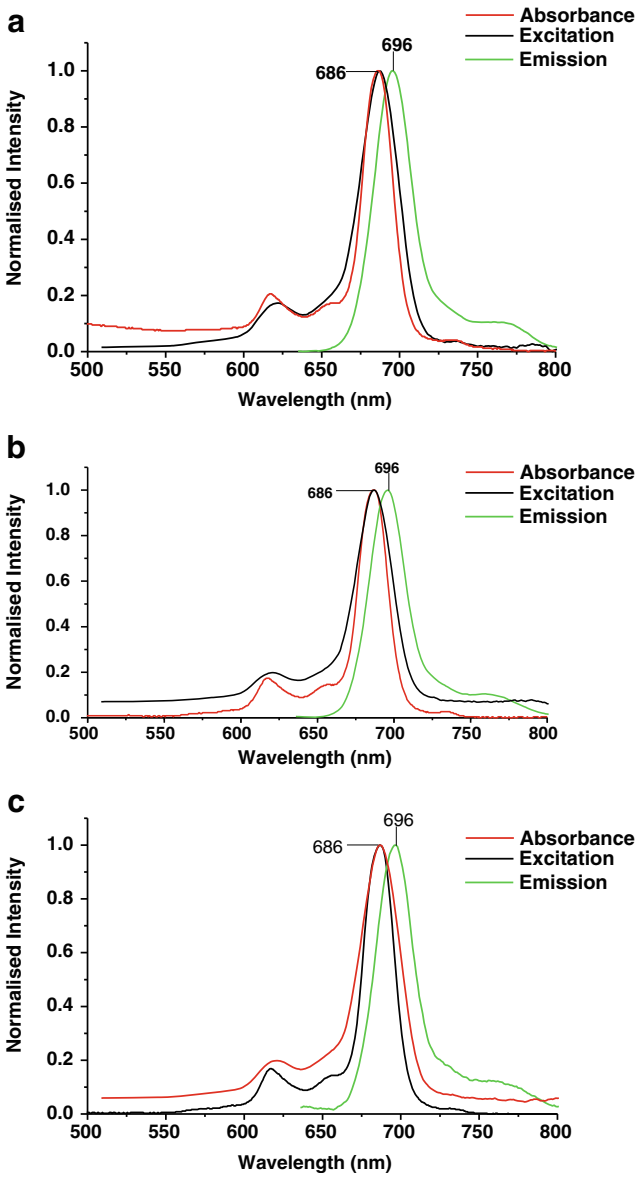

Fig. 5 Absorption, Excitation and Emission spectra of ClAlTSPc in the presence of (**a**) $NaYF_4$:Yb/Er/Gd, (**b**) $NaYF_4$:Yb/Er/Gd@Si and (**c**) $NaYF_4$:Yb/Er/Gd@Si@NH_2. Excitation was at 650 nm in DMSO

DMSO and ethanol) however, the peaks are not as reproducible, hence the UCNPs were embedded in polystyrene fibers as will be discussed in the next section. UCNPs are known to

Table 1 Photophysical parameters of ClAlTSPc in the absence and presence of UCNPs in DMSO

Analysed sample	$\Phi_{F\ (Pc)}$	$\tau_{F\ (Pc)}$ (ns)	$\Phi_{T\ (Pc)}$	$\tau_{T\ (Pc)}$ (μs)
ClAlTSPc alone	0.18	6.51	0.38[a]	103
$NaYF_4$:Yb/Er/Gd@Si/ClAlTSPc	0.15	7.03	0.44	138
$NaYF_4$:Yb/Er/Gd@Si@NH_2/ ClAlTSPc	0.14	7.39	0.52	111

[a] data from reference 35

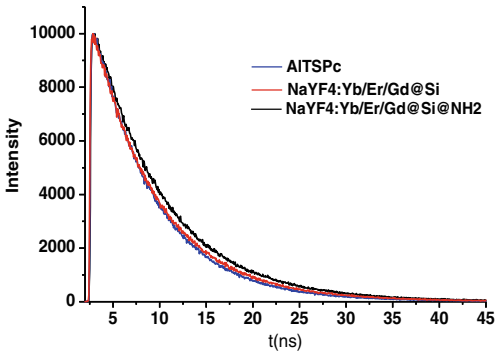

Fig. 6 TCSPC trace of the ClAlTSPc alone and in the presence of $NaYF_4$:Yb/Er/Gd@Si and or $NaYF_4$:Yb/Er/Gd@Si@NH_2 in DMSO. Excitation at 650 nm

suffer from to surface deactivations which have been attributed to surface defects, and to ligands and solvents that possess high phonon energy [15]. In ethanol, the lack of reproducibility of UCNP fluorescence peaks may be attributed to the OH group in ethanol which may facilitate multiphonon relaxations [15]. High phonon energy results in large non-radiative loss and weak upconversion luminescence [38], hence the irreproducible UCNPs emissions in solution could be attributed to non-radiative losses.

Fluorescence Behaviour of UCNPs When Embedded in Fibre, and Suspended in DMSO

The SEM images of the functionalized electrospun PS fibers are shown in Fig. 9. SEM was used to study the size, and the morphology of the functionalized fibers. The fibers obtained were cylindrical, slightly branched with relatively smooth surfaces. The diameters of the fibers ranged from 1 to 5 μm and there was no significant increase on the fiber's diameter upon functionalization with UCNPs. The UCNP fibers are represented with PS at the end of the name in Table 2.

The UCNPs modified electrospun fibers were suspended in DMSO and they did not dissolve. The fluorescence behaviour

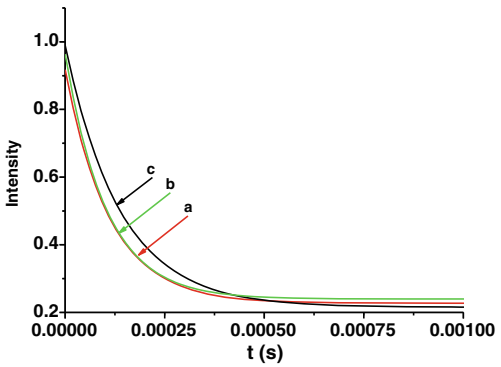

Fig. 7 Triplet decay curve of ClAlTSPc alone (**a**) and in the presence of (**b**) $NaYF_4$:Yb/Er/Gd@Si and (**c**) $NaYF_4$:Yb/Er/Gd@Si@NH_2. Solvent=DMSO

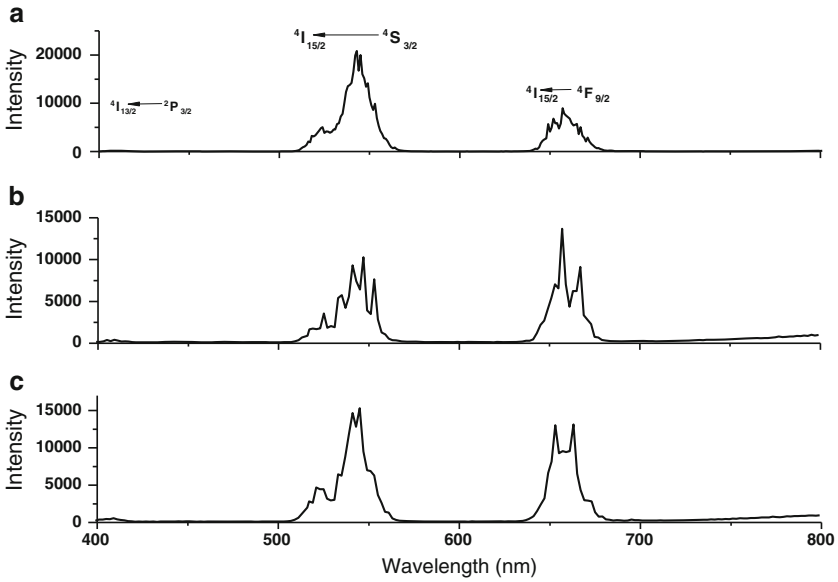

Fig. 8 Fluorescence spectra for (**a**) uncapped $NaYF_4$:Yb/Er/Gd UCNP (1.3×10^{-3} g/ml) in cyclohexane, (**b**) $NaYF_4$:Yb/Er/Gd@Si (6.4×10^{-4} g/ml) in ethanol and (**c**) $NaYF_4$:Yb/Er/Gd@Si@NH_2 (9.5×10^{-4} g/ml) in ethanol

of the UCNPs was investigated when embedded in electrospun fibers and suspended in DMSO in the absence of ClAlTSPc. For these studies, excitation was at 975 nm where UCNPs absorb.

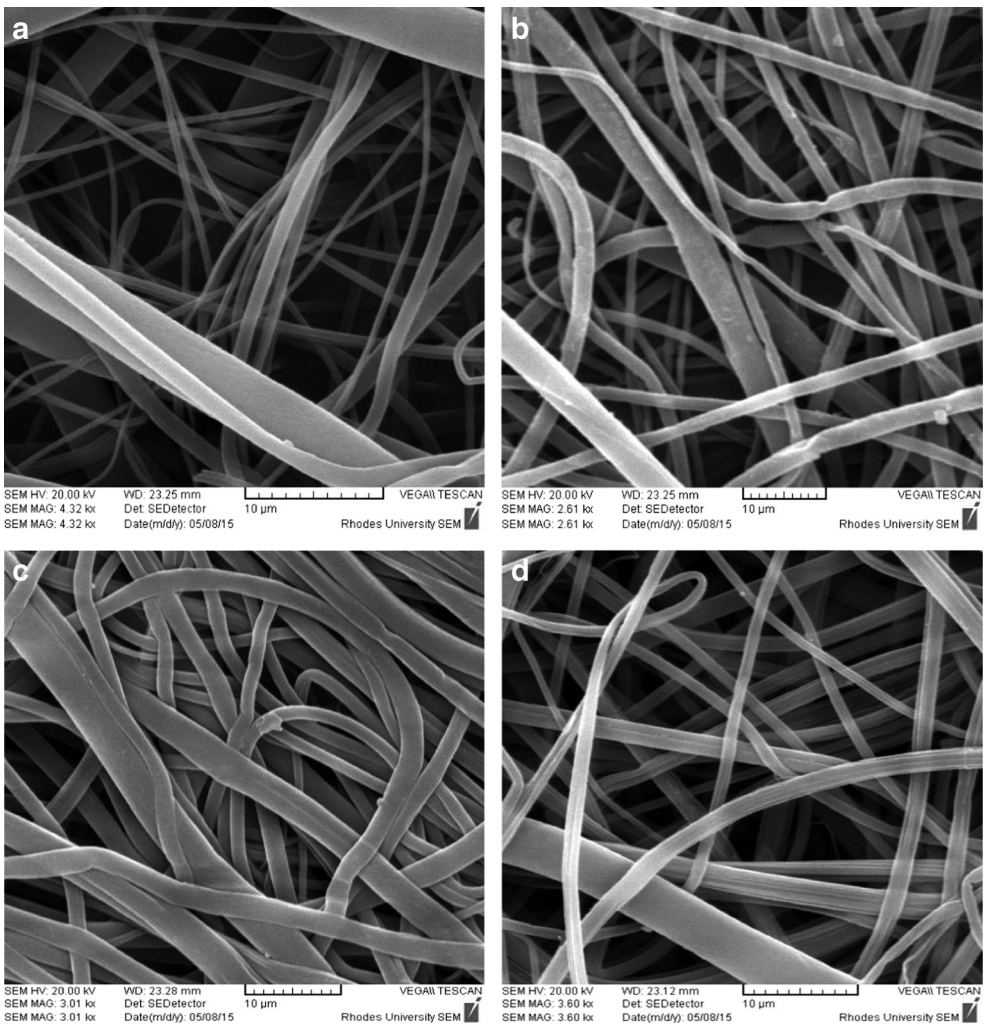

Fig. 9 SEM images of the electrospun polystyrene fibers alone (**a**) in the presence of (**b**) $NaYF_4$:Yb/Er/Gd/PS, (**c**) $NaYF_4$:Yb/Er/Gd@Si/PS and (**d**) $NaYF_4$:Yb/Er/Gd@Si@NH_2/PS UCNPs

Figure 10 shows the emission spectra of the modified fibers suspended in DMSO in the absence of ClAlTSPc. The UCNPs showed intense and incredibly stable fluorescence emissions in the visible region. The emission increased and then stabilized. The peaks in the blue (440 and 488 nm) and far IR (755 nm) regions of the spectrum remain stable while the red (540 nm) and green (658 nm) peaks increased and then stabilized. As stated above, high phonon energy results in large non-radiative loss and weak upconversion luminescence [38]. Thus, the increase in emission intensity for $NaYF_4$:Yb/Er/Gd@Si/PS with time may be due to a decrease in the phonon energy (probably as a result of isolation from solution), resulting in improved fluorescence. Figure 11 compares the fluorescence spectra of uncapped $NaYF_4$:Yb/Er/Gd/PS, $NaYF_4$:Yb/Er/Gd@Si/PS and $NaYF_4$:Yb/Er/Gd@Si@NH_2/PS when suspended in DMSO. Compared to $NaYF_4$:Yb/Er/Gd@Si/PS, uncapped $NaYF_4$:Yb/Er/Gd/PS, and $NaYF_4$:Yb/Er/Gd@Si@NH_2/PS have stronger emission peaks at 440,

Table 2 Absorption spectra and fluorescence data for UCNPs alone, in fibre and in the presence of ClAlTSPc. Excitation was at 975 nm in DMSO

Analysed sample	λ (nm)	τ_{UCNP} (μs)	Error	$\chi 2$	*Eff*
UCNPs not on fiber					
Uncapped $NaYF_4$:Yb/Er/Gd	658	443.7	(±56.9)	0.99	
	540	178.0	(±2.5)	1.05	
$NaYF_4$:Yb/Er/Gd@Si	658	423.0	(±154.0)	0.99	
	540	289.8	(±54.7)	1.03	
$NaYF_4$:Yb/Er/Gd@Si@NH_2	658	323.0	(±288.5)	1.01	
	540	237.0	(±69.0)	0.97	
UCNPs on fiber (suspended in DMSO with or without ClAlTSPc)					
Uncapped $NaYF_4$:Yb/Er/Gd/PS	440	30.2	(±9.5)	1.03	
	488	2.6	(±0.4)	1.16	
	540	13.0	(±7.1)	0.97	
	658	443.7	(±56.9)	0.99	
	755	7.0	(±1.7)	1.16	
Uncapped $NaYF_4$:Yb/Er/Gd/ PS Suspended in DMSO solution of ClAlTSPc	440	36.0	(±18.9)	1.00	
	488	3.8	(±2.3)	1.03	
	540	16.9	(±1.0)	0.97	
	658	a	a	a	a
	755	8.5	(±7.1)	1.00	
$NaYF_4$:Yb/Er/Gd@Si/PS	440	46.3	(±46.8)	1.02	
	488	5.3	(±0.5)	1.03	
	540	250.0	(±37.3)	1.02	
	658	420.6	(±89.5)	0.99	
	755	28.0	(±16.5)	1.01	
$NaYF_4$:Yb/Er/Gd@Si/ PS Suspended in DMSO solution of ClAlTSPc	440	a	a	a	
	488	7.6	(±2.8)	1.01	
	540	141.0	(±120.5)	0.97	
	658	110.9	(±53.9)	1.00	0.74
	755	24.1	(±186.0)	0.97	
$NaYF_4$:Yb/Er/Gd@Si@NH_2/PS	440	33.0	(±27.8)	0.99	
	488	4.8	(±0.6)	1.15	
	540	36.9	(±10.0)	1.03	
	658	51.8	(±18.0)	1.00	
	755	10.5	(±1.8)	1.06	
$NaYF_4$:Yb/Er/Gd@Si@NH_2 /PS Suspended in DMSO solution of ClAlTSPc	440	38.4	(±16.7)	1.00	
	488	7.9	(±1.2)	0.98	
	540	57.0	(±46.1)	1.03	
	658	37.3	(±10.4)	1.18	0.28
	755	17.2	(±8.8)	1.01	

[a] no peak

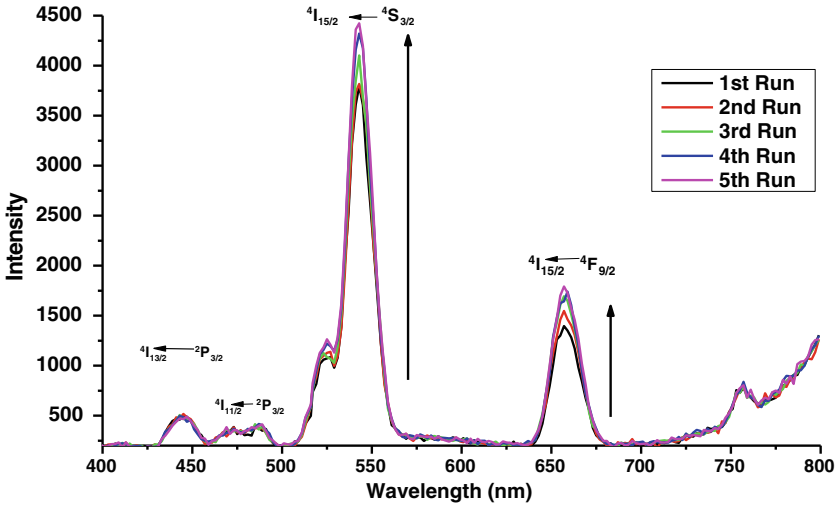

Fig. 10 Fluorescence spectra of $NaYF_4$:Yb/Er/Gd@Si/PS in DMSO

488 and 755 nm and weaker peaks at 540 and 688 nm, where the former had strong emission. There are several factors which affect relative intensities of the UCNP emission peaks such as the size and morphology of the NPs [39] as well as the surface quenching effects [15]. Thus, the changes in the relative intensities of the different UCNPs could be related to some or all of these factors.

Fluorescence Behaviour of UCNPs When Embedded in Fibre, and Suspended in DMSO Containing ClAlTSPc

For these studies, the fluorescence behaviour of the UCNPs was investigated when embedded in electrospun fibers and suspended in DMSO containing ClAlTSPc and excited at 975 nm where UCNPs absorb and ClAlTSPc does not.

The fluorescence lifetimes for $NaYF_4$:Yb/Er/Gd@Si@NH_2/PS and uncapped $NaYF_4$:Yb/Er/Gd/PS increased at all wavelengths (except at 658 nm) in the presence of ClAlTSPc. The decrease in emission at 658 nm which overlaps with the Q band of ClAlTSPc may be attributed to FRET, Table 2.

A decrease in phonon energy results in an increase of the lifetime [40]. Hence the observed increase in lifetimes for some of the wavelengths for $NaYF_4$:Yb/Er/Gd@Si@NH_2/PS and uncapped $NaYF_4$:Yb/Er/Gd/PS in the presence of ClAlTSPc could be related to a decrease in phonon energy as a result of the interaction between the UCNPs embedded in electrospun fiber and ClAlTSPc in solution. For $NaYF_4$:Yb/Er/Gd@Si/PS, there was no emission at 440 nm in the presence of ClAlTSPc, and there was a decrease in emission lifetime at 540, 658 and 755 nm. A decrease in lifetime suggests increased phonon energy or quenching effects in the presence ClAlTSPc. It has been reported before [15] that as the size of the UCNPs decreases, the surface-induced defects increase, resulting in the increase in multiphonon-assisted nonradiative relaxations, which could lead to a decrease in lifetimes. However, the sizes of the three UCNPS are about the same. At 658 nm, FRET is possible due to the overlap of the absorption of ClAlTSPc and the emission of UCNPs, Fig. 11, which is a requirement for FRET and will be discussed below. The decrease in the lifetime at 540 and 755 nm, could not be related to FRET since there is minimal ClAlTSPc absorption at these wavelengths.

For FRET to occur there has to be an overlap between the donor (UCNPs) emission and acceptor (ClAlTSPc) absorption as shown in Fig. 11 for the 658 emission.

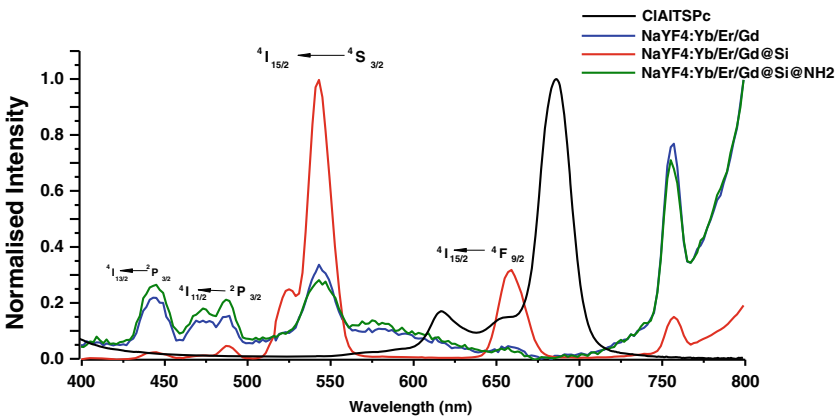

Fig. 11 Absorption Spectrum of ClAlTSPc overlapped with the fluorescence spectra of uncappred $NaYF_4$:Yb/Er/Gd/PS, $NaYF_4$:Yb/Er/Gd@Si/PS and $NaYF_4$:Yb/Er/Gd@Si@NH_2/PS in DMSO

If FRET occurs, there should be a decrease in donor emission and the stimulated emission of the acceptor. From Fig. 12, it is evident that the red emission peak (at 658 nm) of the donor (UCNP) has decreased dramatically in intensity, suggesting the occurrence of FRET. There is only a small increase in background where the ClAlTSPc emission is expect at~690 nm (see Fig. 12). FRET is not the only process that results in the decrease in the donor emission [41, 42], hence the observed weak stimulated emission of ClAlTSPc which does not correspond to the large decrease in UCNP emission. There are many factors other than FRET reported (and are still under debate) that influence photoluminescence decrease in nanoparticles such as quantum dots (QDs) [41–44]. For example, it has been reported that for QD-porphyrin nanocomposites, the major part of the observed quenching of QD photoluminescence can be assigned to non- FRET processes [44]. As already stated, the surface properties and the crystal structure of nanocrystals can change the intensity of UCNP fluorescence peaks [45]. Thus the decrease in the peak intensity of the red peak at 658 nm could also be due to changes in the surface properties of UCNPs embedded in fiber and suspended in ClAlTSPc solution.

The peaks between 400 and 600 nm re-appear for $NaYF_4$:Yb/Er/Gd@Si/PS in the presence of ClAlTSPc, Fig. 12. The increase in the intensity of these peaks could be due to decrease in surface quenching effects of the UCNPs in fiber in the vicinity of ClAlTSPc in solution.

Using Eq. 2, FRET efficiencies for energy transfer from UCNPs to ClAlTSPc following excitation at 975 nm (exciting UCNPs) were estimated to be 0.74 and 0.28 in DMSO, Table 2, for $NaYF_4$:Yb/Er/Gd@Si/PS and $NaYF_4$:Yb/Er/Gd@Si@NH_2/PS, respectively. The larger *Eff* for $NaYF_4$:Yb/Er/Gd@Si/PS/ClAlTSPc is a result of the more intense absorption at 658 nm for $NaYF_4$:Yb/Er/Gd@Si/PS/ClAlTSPc compared to the rest of the UCNPs. For uncapped $NaYF_4$:Yb/Er/Gd/PS, there was no emission at 658 nm in the presence of ClAlTSPc making the estimation of *Eff* difficult.

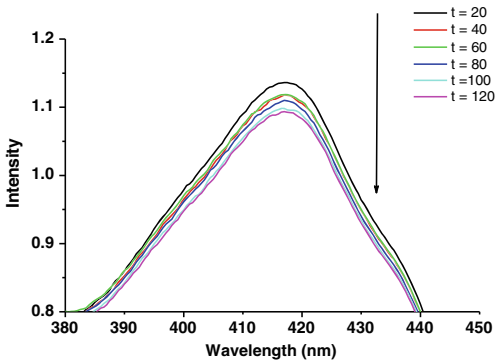

Fig. 13 Degradation profile of DPBF in the presence $NaYF_4$:Yb/Er/Gd@Si/PS suspended in DMSO of ClAlTSPc (7.2×10^{-6} M) containing DPBF ($4.9\times10_{-5}$ M). Time = 0 to 120 min (20 min interval)

Singlet Oxygen Generation by ClAlTSPc in the Presence of UCNPs

UCNPs were embedded in electrospun fibers for these studies and suspended in DMSO solution of ClAlTSPc in order to stabilize the emission of UCNPs, since it is expected that there will be FRET between UCNPs and ClAlTSPc.

Figure 13 shows the degradation profile of DPBF on excitation of $NaYF_4$:Yb/Er/Gd@Si/PS when suspended in DMSO containing DPBF and ClAlTSPc and excited at 975 nm, where UCNPs absorb, but ClAlTSPc does not absorb. There was no decrease in the DPBF absorption for ClAlTSPc alone when irradiation was performed at 975 nm. Thus the decrease in DPBF peak at 418 nm is proof of singlet oxygen generation by ClAlTSPc following excitation of UCNP and energy transfer. When UCNPs (not embedded in fiber) and ClAlTSPc were mixed in DMSO solution, the DPBF peaks were irreproducible.

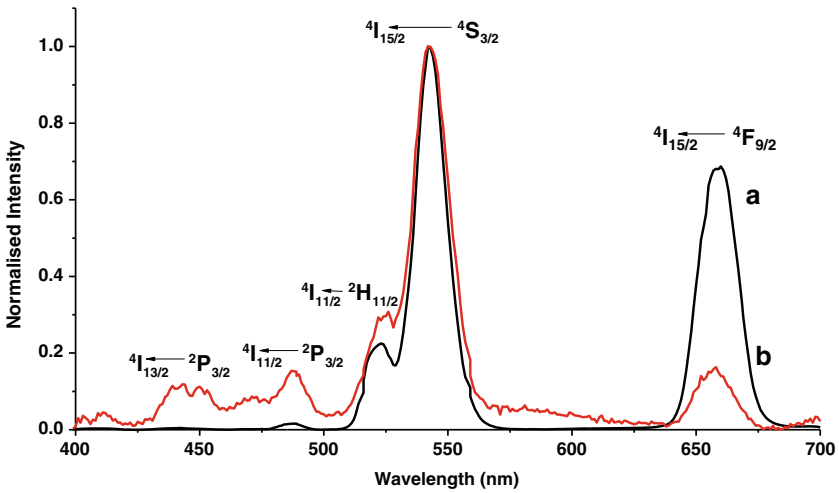

Fig. 12 Fluorescence emission for $NaYF_4$:Yb/Er/Gd@Si/PS (**a**) and $NaYF_4$:Yb/Er/Gd@Si /PS suspended in ClAlTSPc (8.3×10^{-6} M) (**b**) in DMSO

Conclusions

From the data above we can conclude that $NaYF_4$:Yb/Er/Gd upconversion nanoparticles (UCNPs) were synthesised, capped with silica and functionalised with APTES. The photoemission of the UCNPs was stabilised by embedding them in electrospun fibers. The photophysical behaviour of chloro aluminium tetrasulfo phthalocyanines (ClAlTSPc) were studied in the presence of UCNPs. There were no changes in the ClAlTSPc spectra on addition of UCNPs. The Φ_F value of ClAlTSPc in the presence of UCNPs decreased due to the heavy atom effect. Higher triplet quantum yields were observed for ClAlTSPc in the presence of UCNPs as a result of heavy atoms associated with UCNPs. The fluorescence lifetimes (at 658 nm where the emission of UCNPs overlaps with the absorbance of ClAlTSPc) for UCNPs were shortened in the presence of ClAlTSPc due to FRET. The FRET efficiency for $NaYF_4$:Yb/Er/Gd@Si/ClAlTSPc/PS was 0.74 in DMSO while for $NaYF_4$:Yb/Er/Gd@Si@NH_2/ClAlTSPc/PS *Eff*=0.28 in DMSO. A clear singlet oxygen generation by ClAlTSPc though FRET was demonstrated using a singlet oxygen quencher, 1,3-diphenylisobenzofuran in DMSO.

Acknowledgments This work was supported by the Department of Science and Technology (DST)/Nanotechnology (NIC) and National Research Foundation (NRF) of South Africa through DST/NRF South African Research Chairs Initiative for Professor of Medicinal Chemistry and Nanotechnology (UID 62620) and Rhodes University.

References

1. Mckeown NB (1998) Phthalocyanine materials: synthesis, structure and function, chemistry of solid state materials. Cambridge University Press, New York
2. dela Torre G, Vazquez P, Agullo-Lopez F, Torres T (2004) Role of structural factors in the nonlinear optical properties of phthalocyanines and related compounds. Chem Rev 104:3723–3750
3. Erk P, Hengelsberg H (2003) The porphyrin handbook: phthalocyanine dyes and pigments, 19th edn. Academic, San Diego
4. Gregory P (1991) High-technology applications of organic colourant. Plenum Press, New York
5. Nyokong T (2006) In: Zagal JH, Bedioui F, Dodelet JP (eds) Phthalocyanines - properties and applications: electrodes modified with monomeric M-N4 catalysts for the detection of environmentally important molecules. Springer, USA
6. Brozek-Płuska B, Czajkowski W, Kurczewska M, Abramczyk H (2008) Photochemistry of tetrasulphonated magnesium phthalocyanine in water and DMSO solutions by Raman, femtosecond transient absorption, and stationary absorption spectroscopies. J Mol Liq 141:140–144
7. Chin Y, Lim SH, Zorlu Y, Ahsen V, Kiew LV, Chung LY, Dumoulin F, Lee HB (2014) Improved photodynamic efficacy of Zn(II) phthalocyanines via glycerol substitution. PLoS ONE 9:e97894 **(11 pages)**
8. Ben-Hur E, Chan WS (2003) In: Kadish KM, Smith KM, Guilard, R (Eds) The porphyrin handbook: phthalocyanines in photobiology and their medical applications, vol. 19. Academic Press, San Diego, California
9. Bonnett R (2000) Chemical aspects of photodynamic therapy; gordon and breach science. Amsteldijk, The Netherlands
10. Pandey R, Zheng G (2000) In: Kadish KM, Smith KM, Guilard, R (Eds) Pophyrins as photosensitizers in photodynamic therapy, The Porphyrin Handbook, vol. 6. Academic Press
11. Kuznetsova NA, Gretsova NS, Derkacheva VM, Kaliya OL, Lukyanets EA (2003) Sulfonated phthalocyanines: aggregation and singlet oxygen quantum yield in aqueous solutions. J Porphyrins Phthalocyanines 7:147–154
12. Palewska K, Sujka M, Urasińska-Wójcik B, Sworakowski J, Lipiński J, Nešpůrek S, Rakušan J, Karásková M (2008) Light-induced effects in sulfonated aluminum phthalocyanines — potential photosensitizers in the photodynamic therapy. J Photochem Photobiol A 197:1–12
13. DeRosa MC, Crutchley RJ (2002) Photosensitized singlet oxygen and its applications. Coord Chem Rev 233–234:351–371
14. Bejar M, Liras M (2014) NIR excitation of upconversion nanohybrids containing a surface grafted Bodipy induces oxygen-mediated cancer cell death. J Mater Chem B 2:4554–4563
15. Chen G, Qiu H, Prasad PN, Chen X (2014) Upconversion nanoparticles: design, nanochemistry, and applications in theranostics. Chem Rev 114:5161–5214
16. Zhou J, Liu Z, Li F (2012) Upconversion nanophosphors for small-animal imaging. Chem Soc Rev 41:1323–1349
17. Mader HS, Kele P, Saleh SM, Wolfbeis OS (2010) Upconverting luminescent nanoparticles for use in bioconjugation and bioimaging. Curr Opin Chem Biol 14:582–596
18. Idris NM, Jayakumar MKG, Bansal A, Zhang Y (2015) Upconversion nanoparticles as versatile light nanotransducers for photoactivation applications. Chem Soc Rev 44:1449–1478
19. Feng W, Zhu X, Li F (2013) Recent advances in the optimization and functionalization of upconversion nanomaterials for in vivo bioapplications. NPG Asia Mater 5:e75
20. Li X, Zhu J, Man Z, Ao Y, Chen H (2014) Investigation on the structure and upconversion fluorescence of Yb3+/Ho3+ co-doped fluorapatite crystals for potential biomedical applications. Sci Rep 4446, 4 pages
21. Park Y, Nam SH, Kim JH, Bae YM, Yoo B, Kim HM, Jeon K, Park HS, Choi JS, Lee KT, Suh YD, Hyeon T (2013) Comparative study of upconverting nanoparticles with various crystal structures, core/shell structures and surface characteristics. J Phys Chem C 117: 2239–2244
22. Liu M, Liu H, Sun S, Li X, Zhou Y, Hou Z, Lin J (2014) Multifunctional hydroxyapatite/Na(Y/Gd)F4:Yb3+, Er3+ composite fibers for drug delivery and dual modal imaging. Langmuir 30: 1176–1182
23. Bao Y, Luu QAN, Zhao Y, Fong H, May PS, Jiang C (2012) Upconversion polymeric nanofibers containing lanthanide-doped nanoparticles via electrospinning. Nanoscale 4:7369
24. Hou Z, Li X, Li C, Dai Y, Ma P, Zhang X, Kang X, Cheng Z, Lin J (2013) Electrospun upconversion composite fibers as dual drugs delivery system with individual release properties. Langmuir 29: 9473–9482
25. Liu CP, Cheng SH, Chen NT, Lo LW (2012) Intra/inter-particle energy transfer of luminescence nanocrystals for biomedical applications. J Nanomater 706134, 9 pages
26. Qiao X-F, Zhou J-C, Xiao J-W, Wang Y-F, Sun L-D, Yan C-H (2012) Triple-functional core-shell structured upconversion luminescent nanoparticles covalently grafted with photosensitizer for luminescent, magnetic resonance imaging and photodynamic therapy in vitro. Nanoscale 4:4611–4623
27. Zhao Z, Han Y, Lin C, Hu D, Wang F, Chen X, Chen Z, Zheng N (2012) Multifunctional core–shell upconverting nanoparticles for imaging and photodynamic therapy of liver cancer cells. Chem Asian J 7:830–837

28. Sakamoto K, Ohno E (1997) Synthesis and electron transfer property of phthalocyanine derivatives. Prog Org Coat 31:139–145
29. Wang F, Han Y, Lim CS, Lu Y, Wang J, Xu J, Chen H, Zhang C, Hong M, Liu X (2010) Simultaneous phase and size control of upconversion nanocrystals through lanthanide doping. Nature 463:1061–1065
30. Lakowicz JR (1999) Principles of fluorescence spectroscopy, 2nd edn. Kluwer Academic/Plenum Publishers, New York
31. Hsiao J, Krueger BP, Wagner RW, Johnson TE, Delaney JK, Mauzerall DC, Fleming GR, Lindsey JS, Bocian DF, Donohoe RJ (1996) Soluble synthetic multiporphyrin arrays. 2. Photodynamics of energy transfer process. J Am Chem Soc 118:11181–11193
32. Sapra S, Sarma D, Pramana D (2005) Simultaneous control of nanocrystal size and nanocrystal–nanocrystal separation in CdS nanocrystal assembly. Pramana J Phys 65:565–570
33. Fery-Forgues S, Lavabre D (1999) Are fluorescence quantum yields so tricky to measure? A demonstration using familiar stationery products. J Chem Educ 76:1260–1264
34. Nyokong T, Antunes E (2010) In: Kadish KM, Smith KM, Guilard R (Eds) The handbook of porphyrin science, vol 7. Academic Press, New York; World Scientific, Singapore
35. Tran-Thi TH, Desforge C, Thiec C (1989) Singlet-singlet and triplet-triplet intramolecular transfer processes in a covalently linked porphyrin-phthalocyanine heterodimer. J Phys Chem 93: 1226–1233
36. Idowu M, Nyokong T (2007) Photophysical and photochemical properties of zinc and Aluminium phthalocyanines in the presence of magnetic fluid. J Photochem Photobiol A Chem 188:200–206
37. Idowu M, Chen JY, Nyokong T (2008) Photoinduced energy transfer between water soluble CdTe quantum dots and aluminium tetrasulfonated phthalocyanine. New J Chem 32:290–296
38. Wang G, Dai S, Zhang J, Wen L, Yang J, Jiang Z (2005) Intense upconversion luminescence and effect of local environment for Tm3+/Yb3+ co-doped novel TeO2–BiCl3 glass system. Spectrochim Acta A 64:349–354
39. Wang Z, Zeng S, Yu J, Ji X, Zeng H, Xin S, Wang Y, Sun L (2015) Size/morphology induced tunable luminescence in upconversion crystals: ultra-strong single-band emission and underlying mechanisms. Nanoscale. doi:10.1039/c5nr01008j
40. Zhang J, Tao H, Zhao X (2011) Upconversion luminescence properties of Er^{3+} doped GeS_2-Ga_2S_3-KCl chalcohalide glasses. Rare Metals 30:18–21
41. Takanishi CL, Bykova EA, Cheng W, Zheng J (2006) GFP-based FRET analysis in live cells. J Brain Res 1091:132–139
42. Zenkevich EI, Stupak AP, Kowerko D, Borczyskowski C (2012) Influence of single dye molecules on temperature and time dependent optical properties of CdSe/ZnS quantum dots: ensemble and single nanoassembly detection. Chem Phys 406:21–29
43. Blaudeck T, Zenkevich EI, Cichos F, von Borczyskowski C (2008) Probing wave functions at semiconductor quantum-dot surfaces by non-FRET photoluminescence quenching. J Phys Chem C 112: 20251–20257
44. Sun XW, Chen J, Song JL, Zhao DW, Deng WQ, Lei W (2010) Ligand capping effect for dye solar cells with a CdSe quantum dot sensitizd ZnO nanorod photoanode. Opt Express 18:1296–1301
45. Sikora B, Fronc K, Kamińska I, Koper K, Szewczyk S, Paterczyk B, Wojciechowski T, Sobczak K, Minikayev R, Paszkowicz W, Stępień P, Elbaum D (2013) Transport of $NaYF_4$:Er^{3+},Yb^{3+} upconverting nanoparticles into HeLa Cells